International Journal of
Agriculture, Environment and Food Sciences
e-ISSN: 2618-5946 https://dergipark.org.tr/jaefs

DOI: https://doi.org/10.31015/jaefs.2024.3.5 Int. J. Agric. Environ. Food Sci. 2024; 8(3): 521-530

Adsorption of crystal violet dye with selenium nanoparticles obtained by green synthesis from cherry (*Prunus avium* L.) fruit stalk

Alper Solmaz[1] **Talip Turna**[2] **Ayşe Baran**[3]

[1]Department of Environmental Protection and Control-Iskenderun Vocational School of Higher Education, Iskenderun Technical University, Hatay, Turkey
[2]Department of Parks and Garden Plants-Diyarbakır Vocational School of Higher Education, Dicle University, Diyarbakır, Turkey
[3]Department of Biology, Institute of Graduate Studies, Mardin Artuklu University, Mardin, Turkey

Article History
Received: May 12, 2024
Revised: July 25, 2024
Accepted: July 30, 2024
Published Online : July 31, 2024

Artficle Info
Article Type: Research Article
Article Subject: Environmentally Sustainable Engineering

Corresponding Author
Talip Turna
talipturnna@gmail.com

Available at
https://dergipark.org.tr/jaefs/issue/86361/1482849

Abstract

The rapid development of the global production printing and dyeing industry has led to an increase in the demand for various dyes. Crystal violet (CV), a versatile dye, is widely used in the textile industry and other applications. The reason for its widespread use is its effectiveness and the vivid color it gives to fabrics.CV dye is a water-soluble, toxic, resistant organic dye that is quite dangerous for the ecosystem and causes environmental pollution. Therefore, it must be removed before being released into the recipient environment. This study synthesized selenium nanoparticles (Se NPs) from agricultural *Prunus avium* L. (*Pa*L.) wastes and removed CV dye. In batch adsorption tests, the effects of pH, amount of adsorbent, time, initial concentration, and temperature were investigated. In this study, where 3 different kinetic and isotherm models were tested, it was determined that the most suitable kinetic and isotherm models for the removal of CV dye with *Pa*L-Se NPs were Pseudo second order (R^2:0.999) and Langmuir (R^2:0.997), respectively. Additionally, the maximum adsorption capacity (qmax) was calculated as 142.61 mgCV/g *Pa*L-Se NP. Accordingly, it can be said that low-cost *Pa*L-Se NPs synthesized by environmentally friendly methods are a suitable alternative for the removal of CV dye.

Keywords: Agricultural waste, *Prunus avium* L., Green synthesis, Crystal violet, Nanoparticle, Adsorption

Cite this article as: Solmaz, A., Turna, T., Baran, A. (2024). Adsorption of crystal violet dye with selenium nanoparticles obtained by green synthesis from cherry (*Prunus avium* L.) fruit stalk. *International Journal of Agriculture, Environment and Food Sciences*, 2024; 8(3): 521-530. DOI: https://doi.org/10.31015/jaefs.2024.3.5

INTRODUCTION

The acceleration of the production-based economy in the world in the last quarter, together with the progress in science and technology, also accelerated the growth of the textile industry. Due to this rapid growth, dye-based pollution has become a serious environmental problem faced by many developing countries (Ngoc Hoang et al., 2021; Zhao et al., 2019). Synthetic textile wastewater, which contains dyes and has a complex aromatic ring molecular structure, causes harmful effects on the environment and humans, such as allergies, cancer, irritation and even mutations (Du et al., 2011). CV dye, which is included in this toxicological dye group, is a cationic triphenylemethane dye that is widely used in many areas such as textile colorant, paper dye and biological dye (Kulkarni et al., 2017). The presence of the dye in the aquatic ecosystem disrupts the photosynthetic activity of water and affects the fauna and flora of water bodies causing ecological imbalance. For this reason, dye wastewater must be treated before being released into the aquatic ecosystem (Rehan et al., 2023).Therefore, in order to prevent further degradation of the natural ecosystem and protect public health, there is a great need to develop an effective approach to remove dye wastewater prior to discharge into the aquatic ecosystem (Kubra et al., 2021).Removal of azo dyes from wastewater is a major challenge because these dyes have a resistant and complex structure that makes them durable for long periods of time. Thanks to these structures, they are thought to be electron-deficient xenobiotic compounds that are resistant to degradation (Cheruiyot et al., 2019). Many methods such as flocculation, coagulation, membrane filtration, chemical oxidation, ion exchange, electrolysis and reverse osmosis are used for dye removal from aquatic environments (Yagub et al., 2014). In addition to these methods, the adsorption method is one of the most widely used methods in dye removal from aqueous solutions. (Moosavi et al., 2020).Recently, bio-supported production of nanostructured materials (plants, etc.) by researchers has stood

out as environmentally friendly methods that play an important role in minimizing pollution (Rahmat et al., 2023). Physical, chemical or green synthesis (biological methods) methods are used in the synthesis of nanomaterials. However, physical and chemical processes can produce both expensive and toxic products. For this reason, green nanobiotechnology method is frequently used in the production of nanomaterials (Nikam et al., 2022). Nanoparticle-based adsorbents have shown great success in removing dye wastes from aqueous solution due to high surface area, nanoscale size, and chemical composition, among other physical and chemical characteristics (Mashkoor et al., 2020). Therefore, in this study, selenium nanoparticles (*Pa*L-Se NP) were synthesized from agricultural *Prunus avium* L. (*Pa*L.) waste and crystal violet (CV) dye was removed. In batch adsorption tests, the effects of pH, adsorbent amount, time, initial concentration and temperature were investigated, and kinetic and isotherm studies were carried out. Promising results were obtained in the removal of CV dye in this sustainable study, which was carried out as an alternative to other treatment methods.

MATERIALS AND METHODS

Chemicals

All chemicals used in experimental studies are of analytical purity. Powder sodium selenite (Na_2SeO_3, 172.94 g/mol, Sigma-Aldrich), crystal violet dye in powder form ($C_{25}N_3H_{30}Cl$, 407.979 g/mol, Sigma-Aldrich), nitric acid in liquid form (HNO_3, 1.39 g/cm^3, 65%, Merck), sodium hydroxide in pellet form (NaOH, 40.00 g/mol, ≥99.0%, Sigma-Aldrich) and sulfuric acid in liquid form ($H_2(SO_4)_3$, 1.81 g/cm^3, ≥ 90-91 %, Merck) were used.

Collection of *Prunus avium* L. (*Pa*L) Plant

In this study, the stalks of cherries purchased commercially in June in Şeyhan neighborhood of Artuklu district of Mardin province were removed. Later, he was washed many times, first with tap water and then even with pure water. At the end of the process, the cherry stalks were dried in a room protected from sunlight and ground into a powder with a rotary mill (Device name: Ika Universal Muhle). The obtained stalks were stored at +4 ºC to be used in experimental procedures.

Extraction of *Pa*L wastes

In this study, 50 grams of previously dried cherry stalks were weighed. The weighed cherry stalks were placed in a 1000 mL beaker. 400 mL of analytical purity ethanol was added, and it was covered and kept for four days. Then, it was subjected to filtration and the filtrate was removed and the ethanol was removed in a Heidolp brand evaporator. Then, the pure extract remaining at the bottom of the flask was used in experimental procedures(Baran et al., 2023).

Biosynthesis of *Pa*L -Se NPs

500 mg of *Prunus avium* L. (*Pa*L) plant extract, previously pure cherry fruit stalks, were taken into erlenmeayer flask and dissolved in 200 mL of pure water. Then, 150 mL of 75 mM was added from the stock sodium selenite Na_2SeO_3 solution. The reaction process was allowed to stir at 75 ºC for 24 hours. Then, the dark-colored solution was taken and centrifuged (6000 rpm for 25 minutes). After centrifugation, the solid part was removed and placed on a glass pellet and dried at 80 °C for 72 hours. The obtained *Pa*L-SeNPs were preserved to be used in absorption processes. Production stages are presented in Figure 1.

Cherry *Pa*L stalk | Powdered form of *Pa*L stalk | Cherry *Pa*L extract | *Pa*L-SeNPs from *Pa*L | Powder form of *Pa*L-SeNPs stalk

Figure 1. Production scheme showing the synthesis of *Pa*L-SeNPs obtained from *Pa*L stalks

Adsorption studies

First of all, a stock solution of CV dye with a concentration of 1000 mg/L was prepared. Sequential dilute solutions were prepared from this stock solution and a calibration curve was created at a wavelength of 586 nm on a UV-Vis spectrophotometer (Hach DR6000, Germany). The equation y = 0.1871x + 0.0054 (R^2 = 0.9993) was used to measure dye concentrations in adsorption studies. Adsorption studies were carried out in an orbital shaker device (Heidolp, Unimax1010, Germany) at a stirring speed of 200 rpm. In addition, environmental parameters (effect of pH, adsorbent amount, time, and initial concentration) were also studied, and suitable conditions were determined for the adsorption of CV dye on *Pa*L-Se NPs.

Equations (1) and (2) were used to evaluate the numerical data obtained.

$$R(\%) = \frac{C_0 - C_e}{C_0} \times 100 \quad (1)$$

$$q_e = \frac{(C_0 - C_e) \times V}{m} \quad (2)$$

Here, the term *R* refers to the removal efficiency, while the terms C_0 and Ce refer to the dye concentrations (mg/L) at the beginning and end of the reaction, respectively. Additionally, the term *V* represents the solution volume (L) and the term *m* represents the amount of *Pa*L-Se NPs (g).

Adsorption kinetics

Kinetic experiments were conducted at room temperature (23±2 ^{0}C), 200 rpm and neutral pH, in a 50 mL volume beaker with an initial dye concentration of 10 mg/L. Dye concentrations were measured by taking samples at certain intervals and Pseudo first order (equation no. 3) (Lagergren, 1898), Pseudo second order (equation no. 4) (Ho et al., 1996) and Elovich (equation no. 5) (Kumar et al., 2011) models were tried to process the numerical values.

Pseudo first order: non-linear: $\frac{dq_t}{d_t} = K_1(q_e - q_t)$, linear: $Log(q_e - q_t) = Log\ q_e - \frac{K_1}{2.303}t$ (3)

Pseudo second order: non-linear: $\frac{dq_t}{d_t} = K_2(q_e - q_t)^2$, linear: $\frac{t}{q_t} = \frac{1}{K_2 q_e^2} + \frac{1}{q_e}t$ (4)

Elovic: non-linear: $q_t = \beta \ln(\alpha\beta t)$, linear: $q_t = \frac{1}{\beta}\ln(\alpha\beta) + \frac{1}{\beta}\ln t$ (5)

Here, the terms q_e and q_t express the amount of pollutant (mg/g) removed per unit adsorbent at equilibrium and any time *t*, respectively, while K_1 and K_2 are the kinetic constants of the models. Additionally, the term α represents the initial adsorption rate (mg/g.min) and β represents the model constant (g/mg).

Adsorption isotherms

Isotherm experiments were carried out at room temperature (23±2 ^{0}C), 200 rpm and neutral pH 5 mg *Pa*L-Se NPs were added to 6 different tubes with a volume of 10 mL, with initial dye concentration ranging from 15.63 to 500 mg/L, and after centrifugation for 120 minutes, the upper phase water was measured in a UV-Vis spectrophotometer. It was read according to the prepared calibration curve. The obtained numerical values were processed in Freundlich (equation no. 5) (Wang & Guo, 2020), Langmuir (equation no.6) (Guo & Wang, 2019; Langmuir, 1916) and Temkin (equation no.7) (Temkin, 1940) isotherm models.

Freundlich: non-linear: $q_e = k_F C_e^{1/n}$ linear: $log(q_e) = log(k_F) + {}^1/_n\, log(C_e)$ (5)

Langmuir: non-linear: $q_e = \frac{q_m k_L C_e}{1 + k_L C_e}$ linear: $\frac{C_e}{q_e} = \frac{1}{q_{max} k_L} + \frac{C_e}{q_{max}}$ (6)

Temkin: non-linear: $q_e = \frac{RT}{b_T}\, ln(k_T C_e)$ linear: $q_e = \frac{RT}{b_T}\, ln(k_T) + \frac{RT}{b_T}\, ln(C_e)$ (7)

Here, the term q_e represents the amount of pollutant removed per unit adsorbent in equilibrium (mg/g), the term C_e represents the final pollutant concentration (mg/L), and K_f and n represent the Freundlich constants. In the Langmuir isotherm, the term q_m represents the maximum adsorption capacity (mg/g) and K_L represents the Langmuir adsorption constant (L/mg). The equation "$R_L = 1/(1 + a_L.C_0)$" is needed to find the dispersion constant (R_L) in the Langmuir isotherm. Here, the term a_L refers to the Langmuir constant and C_0 refers to the initial pollutant concentration of the reaction (mg/L). Additionally, in the Temkin equation, the term *B* refers to the model constant (J/mol). To calculate this, the equation "$B = R_T/b_T$" is used. Here, the term *R* refers to the universal gas constant (8.314 J/mol. K), the term *T* refers to the temperature (K), and b_T refers to the isotherm constant (kj/mol).

RESULTS AND DISCUSSION

Influence of environmental factors

In order to determine the effect of pH on removing the CV dye of *Pa*L-Se NPs, pH 3, 5, 7 and 9 were used in 4 different tubes with an initial CV concentration of 10 mg/L and an initial amount of *Pa*L-Se NPs of 10 mg, at a stirring speed of 200 rpm at room temperature. Experiments were carried out for 120 minutes. At the end of the period, 7.81, 6.98, 6.92 and 6.88 mg/L dye measurements were observed in the dye measurements made in the upper phase, respectively. In this case, it was determined that the dye removal efficiency reached from 21.9% to 31.2% with increasing pH. In this context, it can be stated that although the removal efficiency is low in strongly acidic conditions, there is an increase in efficiency in neutral pH and partially basic environments, but the

difference is not very high. When the literature was examined, it was reported that the removal efficiency of CV dye was carried out by coating Fe_3O_4 on biochar and that the removal efficiency was suitable at neutral and high pH (Sun et al., 2015). Similarly, in a different study in which CV dye was removed by synthesizing magnetic nanoparticles, it was reported that pH increases positively affected the yield (Samrot et al., 2021).

On the other hand, experiments were carried out under similar environmental conditions to determine in which direction the removal of CV dye was affected by varying amounts of *Pa*L-Se NPs. Again, in 5 different experiments with a volume of 10 mL, where the initial CV concentration was 10 mg/L, 5, 10, 20, 40 and 80 mg *Pa*L-Se NPs were added to each tube, and CV concentrations were measured at the end of the period. According to the data obtained, 84.7% efficiency was achieved at 5 mg dosage, while the efficiency reached 88.2% in the experiment where 10 mg *Pa*L-Se NP was added, and finally, the output dye concentration could not be observed in the experiment where 20 mg *Pa*L-Se NP was added. Therefore, it is clear that the removal efficiency increases as the amount of adsorbent increases. When the literature was examined, it was reported in a study in which CV dye was removed by loading silver nanoparticles on activated carbon that the increase in the amount of adsorbent contributed positively to the removal efficiency (AbdEl-Salam et al., 2017). Similarly, in a different study in which CV dye was removed with photogenic magnetic nanoparticles, it was reported that a decrease in the CV dye output concentration was observed because of the increase in the amount of adsorbent (Ali et al., 2018).

To determine the effect of the initial dye concentration on the removal efficiency in the adsorption process, experiments were carried out in 6 different test tubes with a volume of 10 mL, each with an adsorbent amount of 0.5 g/L, under the same environmental conditions, with the initial dye concentration ranging from 15.63 to 500 mg/L. The data obtained from the dye analyses performed at the end of the period are presented in Figure 2(a). Accordingly, at an initial concentration of 15.63 mg/L, the dye concentration remaining in the solution in the experimental unit was measured as 5.9 mg/L, the removal efficiency was calculated as 62.24% and qe was calculated as 19.45 mg/g. When the initial dye concentration was 125 mg/L, the exit concentration was measured as 68 mg/L, the removal efficiency was calculated as 45.6% and qe was calculated as 114 mg/g. Finally, when the initial dye concentration reached 500 mg/L, the output concentration, removal efficiency and qe values were calculated as 434 mg/L, 13.2% and 132 mg/g, respectively. Accordingly, it is said that the dye removal efficiency is inversely proportional to the increase in the initial dye concentration, while the amount of substance removed per unit adsorbent increased in direct proportion. When the literature was examined, it was reported that similar results were obtained in the removal of CV dye with magnetic nanoparticles (Amodu et al., 2015).

It is very important to determine the effect of contact time on removal efficiency in the adsorption process. To determine this, 25 mg *Pa*L-Se NPs were added to a 50 mL volume beaker with an initial CV concentration of 10 mg/L under the same environmental conditions, samples were taken at certain time intervals and CV dye analysis was performed in the upper phase liquid. The results obtained are presented in Figure 2(b). During the 300-minute experiment period, at the end of the 1st minute, the dye concentration decreased to 5.36 mg/L, in this case, the q*t* value was calculated as 9.28 mg/g and the removal efficiency was calculated as 46.4%. While no significant decrease was observed in the exit dye concentration as the reaction time was extended, the CV concentration was measured as 3.57 mg/L at the end of 300 minutes, the qt value was 12.86 mg/g and the removal efficiency was calculated as 64.3%. When the literature was examined, it was determined that CV and MB dyes were removed by synthesizing magnetic iron oxide nanoparticles from fig leaves, and a decrease in dye concentration was observed as the reaction time increased (Alizadeh et al., 2017).

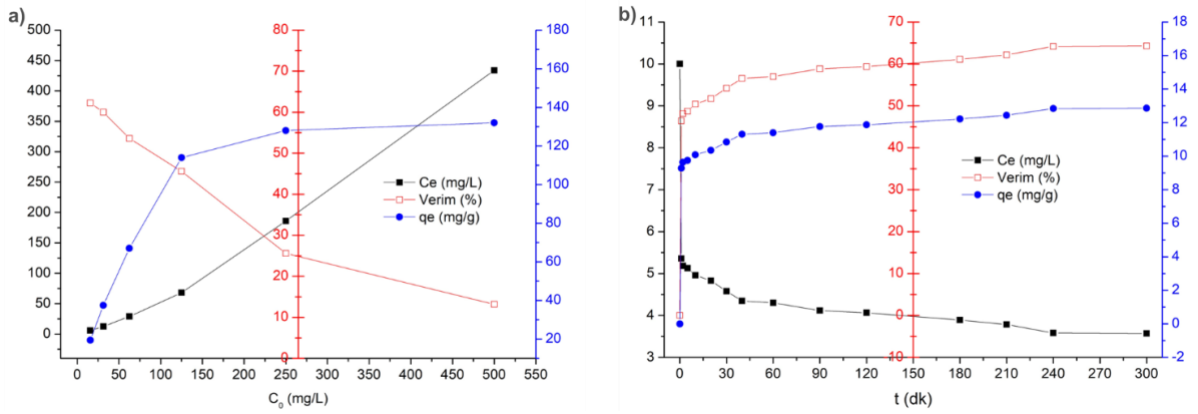

Figure 2. a) Effect of initial concentration; C_0:15.63-500 mg/L, V: 10 mL, m: 0.5 g/L, pH 7.0, T: 23^{0}C, mixing 200 rpm, Time: 120 min, b) Effect of contact time, V: 50 mL, m: 0.5 g/L, C_0:10 mg/L, pH 7.0, T: 23^{0}C, stirring 200 rpm.

Adsorption kinetics

To determine which of the Pseudo first order, Pseudo second order and Elovich kinetic models the numerical data obtained in the experiments conducted in the laboratory fit, the data obtained by removing the linear regression curves of the models are shown in Table 1 and Figure 3(a), (b) and (c). is also presented. In addition, the graph showing the change in time of the amounts of pollutants removed per unit adsorbent obtained from laboratory experiments and the values obtained from kinetic models is presented in Figure 3(d).

Thanks to kinetic models, information is obtained about how long it takes the adsorbent to remove the pollutant it is intended to remove. In addition, information is obtained about the step of the adsorbent in adsorbing the pollutant. The R^2 value is generally considered to determine which kinetic, and isotherm model the numerical data obtained from experimental studies are suitable for. When the table is examined, the R^2 values of the Pseudo first order and Elovich kinetic models were calculated as 0.962 and 0.947, respectively, while the R^2 value of the Pseudo second-order kinetic model was calculated as 0.999. Accordingly, the adsorption process of *Pa*L-Se NP particles to the CV dye occurs following the Pseudo second-order kinetic model. When the literature was examined, the removal of CV dye was achieved with nanoparticles obtained from corn starch and it was reported that it fit the Pseudo second order kinetic model with an R^2 value of 0.999 (Gad et al., 2019). On the other hand, in a study in which carbon nanotubes and nanoparticles were synthesized and the CV dye was removed, it was found that there was a Pseudo second order kinetic model with an R^2 value of 0.999 (Gabal et al., 2014). In another study, cv dye removal from aqueous solution was examined using a surfactant-modified magnetic nanoadsorbent and it was reported that it fit the Pseudo second-order kinetic model with an R^2 value of 0.993 (Muthukumaran et al., 2016).

In another reported study CV dye removal from aqueous solution was examined using *Spirulina*-based surfactant-modified iron oxide nanoparticles for the adsorptive removal of CV dye, and it was stated that it fit the Pseudo second-order kinetic model with an R^2 value of 0.964 (Bhukal et al., 2022).

Table 1. Kinetic and isotherm parameters were calculated for the adsorption of CV on *Pa*L-Se NPs.

		Parameter		R^2
Kinetic models	Pseudo first order	k_1 = 0.052		0 .962
	Pseudo second order	k_2 = 0.034	q_e = 12.407	0 .999
	Elovich	β = 1.544	α = 587384	0 .947
Isotherm models	Freundlich	k_F = 11,986	1/n = 0.447	0 .844
	Langmuir	k_L = 0.034	R_L = 0.172 q_{max} = 142.61	0 .997
	Temkin	B_T = 0.085	k_T = 0.374	0 .921

Adsorption isotherms

To determine the most appropriate isotherm model for the adsorption of CV dye on *Pa*L-Se NPs, calculations of Freundlich, Langmuir and Temkin models were made and presented in Table 1. In addition, linear regression curves were created and shown in Figure 4(a), (b) and (c), and the change of experimental and theoretical qt values against Ce values is shown in Figure 4(d).

In this context, the R^2 values of the Freundlich and Temkin isotherm models were calculated as 0.844 and 0.921, respectively, while the R^2 value of the Langmuir isotherm model was calculated as 0.997. Additionally, the maximum adsorption amount was calculated as 142.61 mg/g. Accordingly, it seems that the most suitable model for the adsorption of CV dye on *Pa*L-Se NPs is Langmuir. In the Langmuir isotherm model, it can be said that the adsorption process occurs in certain localized regions and there is single-layer adsorption (Vijayaraghavan et al., 2006). When the literature was examined, the removal of CV dye was achieved by obtaining nickel oxide nanocomposite with various nickel compounds, and it was reported that the most suitable model was Langmuir with an R^2 value of 0.999 and a q_{max} value of 53.16 mg/g (Bani-Fwaz et al., 2021). On the other hand, in a study in which F_3O_4 nanoparticle synthesis was carried out from weathered basalt stones, the CV dye was removed, and it was reported that the most suitable model was the Langmuir model with an R^2 value of 0.967 and a q_{max} value of 282.5 mg/g (Abu Sharib et al., 2021).

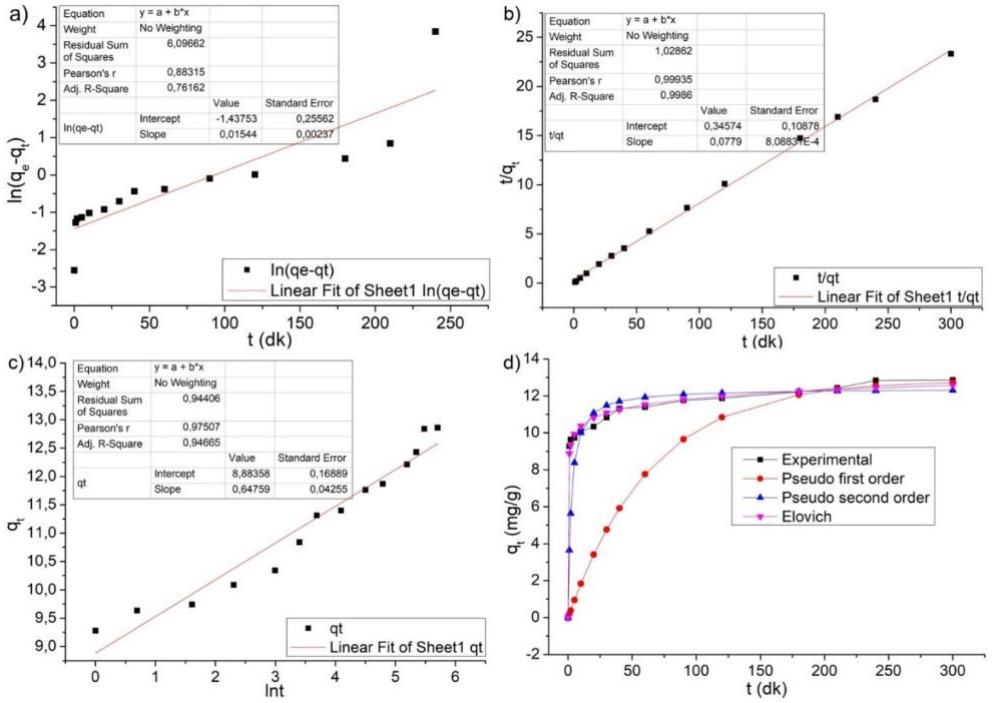

Figure 3. a) Pseudo first order model, b) Pseudo second order model, c) Elovic model, d) change graph of experimental and theoretical q_t values against t.

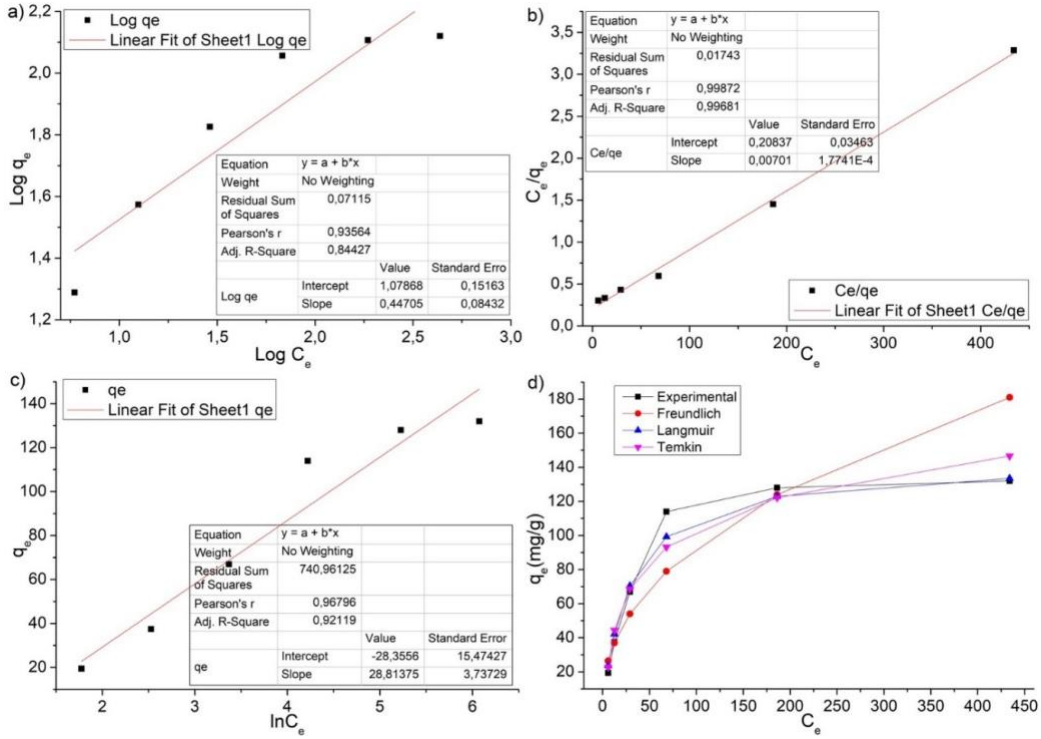

Figure 4. Regression curves of each isotherm model (a) Freundlich, b) Langmuir, c) Temkin and d) Variation of experimental and theoretical q_t values against C_e values.

Comparison of the study and the results obtained with the literature

A summary of the experimental conditions and results of this study is presented in Table 2, along with a comparison of similar studies in the literature. In the study carried out for the purpose of adsorption of CV onto functionalized multi-walled carbon nanotubes, it showed good agreement with langmuir and freundlich isotherm models and pseudo-second-order kinetic model; the maximum adsorption capacity was 90.52 mg/g (Sabna et al., 2016). In the study in which CV dye was removed with the nanomaterial obtained from chitin shrimp shell, the removal efficiency 79.13% and adsorption capacity were found to be 39.56 mg/g (Gopi et al., 2016). To remove the Congo red (CR) dye, zinc oxide (ZnO) in nanoflake form on the zeolite surface was used. In a different adsorption study, it was determined that the most suitable kinetic model was the pseudo-second order kinetic model, and the most suitable isotherm model was the langmuir isotherm model, and the maximum adsorption capacity was 161.3 mg/g (Madan et al., 2019). In a study in which CV dye was removed with *Citrus Fortinella*-Se NPs, it was determined that the most appropriate kinetic model was the pseudo-second order kinetic model with an R^2 value of 0.999, and the most appropriate isotherm model was freundlich with an R^2 value of 0.993. The maximum adsorption capacity was 23.55 mg/g (Solmaz et al., 2024). In this study, it was determined that the most suitable kinetic model was the pseudo-second order kinetic model with an R^2 value of 0.999, and the most suitable isotherm model was the langmuir isotherm model with an R^2 value of 0.997. The maximum adsorption capacity was 142.65 mg/g. As a result, the *Pa*L-Se NPs used in our study are seen as promising for environmental studies due to their adsorption capacity and environmental friendliness.

Table 2. Comparison of the results obtained with the literature.

	This study	(Sabna et al., 2016)	(Gopi et al., 2016)	(Madan et al., 2019)	(Solmaz et al., 2024)
NP Chemical	Se	Commercial product	Chitin-Fe_3O_4	ZnO	Se
NP Origin	*prunus avium*	multi-walled carbon nanotubes	shrimp shell	silica zeolitic	*citrus fortunella*
Experiment volume (mL)	50	20	40	50	50
Mixing speed (rpm)	200	-	600	-	200
Experiment time (min)	120	45	-	60	1500
Working pH's	3-9	3-8	-	3-12	7.0±0.5
pH adjusting agent	0.1 M H_2SO_4/NaOH	-	-	-	0.1 M H_2SO_4/NaOH
Working temperature (^{0}C)	23±2	-	Room	Room	23±2
Removed pollutant	CV	CV	CV	CR	CV
Working pollutants concentrations (mg/L)	15.63-500	25-150	-	25-500	6.25-200
Adsorbent amount (g/L)	0.5	0.25-1.25	-	0.025– 0.1 g	-
Best fitted kinetic model	pseudo-second-order	pseudo-second-order	-	pseudo-second-order	pseudo-second-order
Best fitted isotherm model	Langmuir	Langmuir-Freundlich	-	Langmuir	Freundlich
Max. adsorption capacity (mg/g)	142.61	90.52	39.56	161.3	23.55

CONCLUSION

In this study, the removal of CV dye was carried out with *Pa*L-Se synthesized from agricultural *Pa*L wastes. The effects of pH, adsorbent amount, initial dye concentration and contact time on CV dye removal were discussed. By comparing the values derived from the linear forms of 3 different isotherms and kinetic models, The most suited kinetic model was found to be Pseudo second order, and the most appropriate isotherm model was Langmuir. On the other hand, the maximum CV removal amount of *Pa*L-Se NPs was calculated as 142.61 mgCV/g *Pa*L-Se NPs. Studies were carried out between pH 3-9 to determine the effect of pH on the removal of CV dye from PaL-Se NPs. Additionally, studies were performed between pH 3-9 to determine the effect of pH on the removal of CV dye from PaL-Se NPs. In this case, it was determined that as the pH increased, the dye removal efficiency reached from 21.9% to 31.2%. Overall, these results indicate that green synthesis of selenium nanoparticles has the potential to be an effective, economical and environmentally friendly method for many scientific and technical applications in the future for the treatment of organic dye pollution in aquatic ecosystems.

Compliance with Ethical Standards

Peer-review

Externally peer-reviewed.

Declaration of Interests

The authors declare that they have no competing, actual, potential or perceived conflict of interest

Author contribution

The contribution of the authors to the present study is equal. All the authors read and approved the final manuscript. All the authors verify that the text, figures, and tables are original and that they have not been published before.

Funding

No financial support was received for this study.

REFERENCES

AbdEl-Salam, A. H., Ewais, H. A., & Basaleh, A. S. (2017). Silver nanoparticles immobilised on the activated carbon as efficient adsorbent for removal of crystal violet dye from aqueous solutions. A kinetic study. *Journal of Molecular Liquids*, *248*, 833–841. https://doi.org/10.1016/j.molliq.2017.10.109

Abu Sharib, A. S. A. A., Bonilla-Petriciolet, A., Selim, A. Q., Mohamed, E. A., & Seliem, M. K. (2021). Utilizing modified weathered basalt as a novel approach in the preparation of Fe3O4 nanoparticles: Experimental and theoretical studies for crystal violet adsorption. *Journal of Environmental Chemical Engineering*, *9*(6), 106220. https://doi.org/10.1016/j.jece.2021.106220

Ali, I., Peng, C., Khan, Z. M., Sultan, M., & Naz, I. (2018). Green Synthesis of Phytogenic Magnetic Nanoparticles and Their Applications in the Adsorptive Removal of Crystal Violet from Aqueous Solution. *Arabian Journal for Science and Engineering*, *43*(11), 6245–6259. https://doi.org/10.1007/s13369-018-3441-6

Alizadeh, N., Shariati, S., & Besharati, N. (2017). Adsorption of Crystal Violet and Methylene Blue on Azolla and Fig Leaves Modified with Magnetite Iron Oxide Nanoparticles. *International Journal of Environmental Research*, *11*(2), 197–206. https://doi.org/10.1007/s41742-017-0019-1

Amodu, O. S., Ojumu, T. V., Ntwampe, S. K., & Ayanda, O. S. (2015). Rapid Adsorption of Crystal Violet onto Magnetic Zeolite Synthesized from Fly Ash and Magnetite Nanoparticles. *Journal of Encapsulation and Adsorption Sciences*, *05*(04), 191–203. https://doi.org/10.4236/jeas.2015.54016

Bani-Fwaz, M. Z., El-Zahhar, A. A., Abd-Rabboh, H. S. M., Hamdy, M. S., & Shkir, M. (2021). Synthesis of NiO nanoparticles by thermal routes for adsorptive removal of crystal violet dye from aqueous solutions. *International Journal of Environmental Analytical Chemistry*, *101*(8), 1126–1144. https://doi.org/10.1080/03067319.2019.1678599

Baran, M. F., Keskin, C., Baran, A., Kurt, K., İpek, P., Eftekhari, A., Khalilov, R., Fridunbayov, I., & Cho, W. C. (2023). Green synthesis and characterization of selenium nanoparticles (Se NPs) from the skin (testa) of Pistacia vera L. (Siirt pistachio) and investigation of antimicrobial and anticancer potentials. *Biomass Conversion and Biorefinery*. https://doi.org/10.1007/s13399-023-04366-8

Bhukal, S., Sharma, A., Rishi, Divya, Kumar, S., Deepak, B., Pal, K., & Mona, S. (2022). Spirulina Based Iron Oxide Nanoparticles for Adsorptive Removal of Crystal Violet Dye. *Topics in Catalysis*, *65*(19–20), 1675–1685. https://doi.org/10.1007/s11244-022-01640-3

Cheruiyot, G. K., Wanyonyi, W. C., Kiplimo, J. J., & Maina, E. N. (2019). Adsorption of toxic crystal violet dye using coffee husks: Equilibrium, kinetics and thermodynamics study. *Scientific African*, *5*, e00116. https://doi.org/10.1016/j.sciaf.2019.e00116

Du, J.-J., Yuan, Y.-P., Sun, J.-X., Peng, F.-M., Jiang, X., Qiu, L.-G., Xie, A.-J., Shen, Y.-H., & Zhu, J.-F. (2011). New photocatalysts based on MIL-53 metal–organic frameworks for the decolorization of methylene blue dye. *Journal of Hazardous Materials*, *190*(1–3), 945–951. https://doi.org/10.1016/j.jhazmat.2011.04.029

Gabal, M. A., Al-Harthy, E. A., Al Angari, Y. M., & Abdel Salam, M. (2014). MWCNTs decorated with Mn0.8Zn0.2Fe2O4 nanoparticles for removal of crystal-violet dye from aqueous solutions. *Chemical Engineering Journal*, *255*, 156–164. https://doi.org/10.1016/j.cej.2014.06.019

Gad, E., Owda, M., Mousa, R., & Abdelhai, F. (2019). A Novel Starch Nanoparticle Citrate based Adsorbent for removing of Crystal Violet dye from aqueous solution. *Egyptian Journal of Chemistry*, *0*(0), 0–0. https://doi.org/10.21608/ejchem.2019.16593.2013

Gopi, S., Pius, A., & Thomas, S. (2016). Enhanced adsorption of crystal violet by synthesized and characterized chitin nano whiskers from shrimp shell. *Journal of Water Process Engineering*, *14*, 1–8. https://doi.org/10.1016/j.jwpe.2016.07.010

Guo, X., & Wang, J. (2019). Comparison of linearization methods for modeling the Langmuir adsorption isotherm. *Journal of Molecular Liquids*, *296*, 111850. https://doi.org/10.1016/j.molliq.2019.111850

Ho, Y. S., Wase', D., & Forster, C. F. (1996). Removal of lead ions from aqueous solution using sphagnum moss peat as adsorbent. *Water SA*, *22*(3), 214–219.

Kubra, K. T., Salman, Md. S., & Hasan, Md. N. (2021). Enhanced toxic dye removal from wastewater using biodegradable polymeric natural adsorbent. *Journal of Molecular Liquids*, *328*, 115468. https://doi.org/10.1016/j.molliq.2021.115468

Kulkarni, M. R., Revanth, T., Acharya, A., & Bhat, P. (2017). Removal of Crystal Violet dye from aqueous solution using water hyacinth: Equilibrium, kinetics and thermodynamics study. *Resource-Efficient Technologies*, *3*(1), 71–77. https://doi.org/10.1016/j.reffit.2017.01.009

Kumar, P. S., Ramalingam, S., Kirupha, S. D., Murugesan, A., Vidhyadevi, T., & Sivanesan, S. (2011). Adsorption behavior of nickel(II) onto cashew nut shell: Equilibrium, thermodynamics, kinetics, mechanism and process design. *Chemical Engineering Journal*, *167*(1), 122–131. https://doi.org/10.1016/J.CEJ.2010.12.010

Lagergren, S. K. (1898). About the theory of so-called adsorption of soluble substances. *Sven. Vetenskapsakad. Handingarl*, *24*, 1–39.

Langmuir, I. (1916). The constitution and fundamental properties of solids and liquids. Part I. Solids. *Journal of the American Chemical Society*, *38*(11), 2221–2295. https://doi.org/10.1021/JA02268A002/ASSET/JA02268A002.FP.PNG_V03

Madan, S., Shaw, R., Tiwari, S., & Tiwari, S. K. (2019). Adsorption dynamics of Congo red dye removal using ZnO functionalized high silica zeolitic particles. *Applied Surface Science*, *487*, 907–917. https://doi.org/10.1016/j.apsusc.2019.04.273

Mashkoor, F., Nasar, A., & Inamuddin. (2020). Carbon nanotube-based adsorbents for the removal of dyes from waters: A review. *Environmental Chemistry Letters*, *18*(3), 605–629. https://doi.org/10.1007/s10311-020-00970-6

Moosavi, S., Lai, C. W., Gan, S., Zamiri, G., Akbarzadeh Pivehzhani, O., & Johan, M. R. (2020). Application of Efficient Magnetic Particles and Activated Carbon for Dye Removal from Wastewater. *ACS Omega*, *5*(33), 20684–20697. https://doi.org/10.1021/acsomega.0c01905

Muthukumaran, C., Sivakumar, V. M., & Thirumarimurugan, M. (2016). Adsorption isotherms and kinetic studies of crystal violet dye removal from aqueous solution using surfactant modified magnetic nanoadsorbent. *Journal of the Taiwan Institute of Chemical Engineers*, *63*, 354–362. https://doi.org/10.1016/j.jtice.2016.03.034

Ngoc Hoang, B., Thi Nguyen, T., Van Nguyen, D., & Van Tan, L. (2021). Removal of crystal violet from aqueous solution using environment-friendly and water-resistance membrane based on polyvinyl/agar/maltodextrin. *Materials Today: Proceedings*, *38*, 3046–3052. https://doi.org/10.1016/j.matpr.2020.09.391

Nikam, P. B., Salunkhe, J. D., Minkina, T., Rajput, V. D., Kim, B. S., & Patil, S. V. (2022). A review on green synthesis and recent applications of red nano Selenium. *Results in Chemistry*, *4*, 100581. https://doi.org/10.1016/j.rechem.2022.100581

Rahmat, M., Kiran, S., Gulzar, T., Yusuf, M., Nawaz, R., Khalid, J., Fatima, N., Ullah, A., & Azam, M. (2023). Plant-assisted synthesis and characterization of MnO2 nanoparticles for removal of crystal violet dye: an environmental remedial approach. *Environmental Science and Pollution Research*, *30*(20), 57587–57598. https://doi.org/10.1007/s11356-023-26601-5

Rehan, A. I., Rasee, A. I., Awual, M. E., Waliullah, R. M., Hossain, M. S., Kubra, K. T., Salman, Md. S., Hasan, Md. M., Hasan, Md. N., Sheikh, Md. C., Marwani, H. M., Khaleque, Md. A., Islam, A., & Awual, Md. R. (2023). Improving toxic dye removal and remediation using novel nanocomposite fibrous adsorbent. *Colloids and Surfaces A: Physicochemical and Engineering Aspects*, *673*, 131859. https://doi.org/10.1016/j.colsurfa.2023.131859

Sabna, V., Thampi, S. G., & Chandrakaran, S. (2016). Adsorption of crystal violet onto functionalised multi-walled carbon nanotubes: Equilibrium and kinetic studies. *Ecotoxicology and Environmental Safety*, *134*, 390–397. https://doi.org/10.1016/j.ecoenv.2015.09.018

Samrot, A. V., Ali, H. H., Selvarani A, J., Faradjeva, E., P, R., P, P., & Kumar S, S. (2021). Adsorption efficiency of chemically synthesized Superparamagnetic Iron Oxide Nanoparticles (SPIONs) on crystal violet dye. *Current Research in Green and Sustainable Chemistry*, *4*, 100066. https://doi.org/10.1016/j.crgsc.2021.100066

Solmaz, A., Turna, T., & Baran, A. (2024). Ecofriendly synthesis of selenium nanoparticles using agricultural <scp> *Citrus fortunella* </scp> waste and decolourization of crystal violet from aqueous solution. *The Canadian Journal of Chemical Engineering*, *102*(6), 2051–2067. https://doi.org/10.1002/cjce.25179

Sun, P., Hui, C., Azim Khan, R., Du, J., Zhang, Q., & Zhao, Y.-H. (2015). Efficient removal of crystal violet using Fe3O4-coated biochar: the role of the Fe3O4 nanoparticles and modeling study their adsorption behavior. *Scientific Reports*, *5*(1), 12638. https://doi.org/10.1038/srep12638

Temkin, M. I. (1940). Kinetics of ammonia synthesis on promoted iron catalysts. *Acta Physiochim*, *12*, 327–356.

Vijayaraghavan, K., Padmesh, T., Palanivelu, K., & Velan, M. (2006). Biosorption of nickel(II) ions onto Sargassum wightii: Application of two-parameter and three-parameter isotherm models. *Journal of Hazardous Materials*, *133*(1–3), 304–308. https://doi.org/10.1016/j.jhazmat.2005.10.016

Wang, J., & Guo, X. (2020). Adsorption isotherm models: Classification, physical meaning, application and solving method. *Chemosphere*, *258*, 127279. https://doi.org/10.1016/J.CHEMOSPHERE.2020.127279

Yagub, M. T., Sen, T. K., Afroze, S., & Ang, H. M. (2014). Dye and its removal from aqueous solution by adsorption: A review. *Advances in Colloid and Interface Science*, *209*, 172–184. https://doi.org/10.1016/j.cis.2014.04.002

Zhao, X., Chen, H., Kong, F., Zhang, Y., Wang, S., Liu, S., Lucia, L. A., Fatehi, P., & Pang, H. (2019). Fabrication, characteristics and applications of carbon materials with different morphologies and porous structures produced from wood liquefaction: A review. *Chemical Engineering Journal*, *364*, 226–243. https://doi.org/10.1016/j.cej.2019.01.159